EUROPEAN ORGANIZATION FOR NUCLEAR RESEARCH

CERN-PPE/96-07
16 January 1996

# The L3 lead-scintillating fiber calorimeter

G. Basti, M. Campanelli[a)], F. Cavallari, F. de Notaristefani[b)], M. Diemoz, R. Faccini, F. Ferroni, A. Iaciofano, E. Leonardi, E. Longo, G. Organtini[b)], S. Paoletti
Università di Roma "La Sapienza" and INFN - Sez. di Roma, P.le A. Moro 2 -00185 Roma, Italy

A. Boucham, B. Camberlin, Y. Karyotakis, J. Lesueur
Laboratoire d'Annecy-le-Vieux de Physique des Particules, LAPP,IN2P3-CNRS, BP 110, F-74941 Annecy-le-Vieux CEDEX, France

C. Cecchi
University of Geneva, CH-1211 Geneva 4, Switzerland

M. Lebeau
CERN, CH-1211 Geneva 23, Switzerland

Y. Tsipolitis
Carnegie Mellon University, Pittsburgh, PA 15213, USA

## Abstract

We report on the construction and test of a lead-scintillating fiber (*spaghetti*) calorimeter built to fill the gap between endcaps and barrel in the L3 BGO detector. Results from test-beam, as well as MC simulations for the prototypes and for the full detector, are presented.

*(submitted to NIM)*

[a)] Now at ETH, Zurich, Switzerland.
[b)] Now at Univ. di Roma III, Rome, Italy.

## 1 Introduction

The L3 BGO electromagnetic calorimeter [1] consists of a central (barrel) and two forward-backward (endcap) regions. They are separated by a gap without electromagnetic coverage, for polar angles $38^\circ < \theta < 42^\circ$ and $138^\circ < \theta < 142^\circ$. This dead zone causes a loss of statistics and an increase of systematic uncertainties for most processes, and an increase of background for new particle searches. In particular, a radiative Bhabha event with the photon pointing to the gap could generate momentum imbalance, which is the main signature for production of SUSY particles [2]. This background can become important as the number of SUSY events expected at LEP2 energy is very low. For these reasons L3 decided to build a lead-scintillating fiber electromagnetic calorimeter to be placed in the BGO gap.

This paper describes the design of the calorimeter and the results obtained with prototype modules at test beams, as well as MC simulations of the expected performance.

## 2 Calorimeter design

The new detector is composed of two parts, one for each gap, each made of 24 modules of trapezoidal shape mounted side by side to fit in the gap (see Fig.1). Some space is left between the modules for 24 groups of cables coming from the inner tracking detector (TEC). In order to minimize the inefficiency of the calorimeter, the gap between modules is not pointing to the interaction point, but is tilted by about $25^\circ$.

Views of a module are shown in Fig. 2. Each module, or brick, is made of a lead structure filled with scintillating fibers with their axes along the brick main axis. The ratio in volume between lead and fibers is 4:1, giving $X_0 = 0.72$ cm, in order to ensure a sufficient shower containment ($21X_0$) in the reduced space left between TEC and the hadronic calorimeter. Light collection is performed by two plexiglass light guides per module. It was not possible in fact to convey the fibers directly to the photon detectors because the rear shower leakage produced signals in those fibers.

To study the performances of different types of light guide, a test bench was set up. Light pulses were sent from an LED to the light guide face through a fiber, and the light from the guide was read by a photomultiplier tube. The whole face of the light guide was scanned by means of a computer-controlled system of step-motors and the pulse height as a function of the position of the fiber with respect to the guide was digitized by an ADC and recorded on a PC. Results of a scan along the largest axis (horizontal axis) of different lightguide prototypes are shown in Fig. 3. It can be concluded that plexiglass lightguides are the best solution both in terms of spatial uniformity and light collection efficiency.

Since the modules form a $40^\circ$ angle with respect to the 0.5 T magnetic field, photomultipliers cannot be used in the final setup; the readout was done by Hamamatsu R2148 phototriodes. An LED system is used for phototriode monitoring.

The rear part of each module, containing the triodes, the lightguides, the calibration LEDs and two preamplifiers, is enclosed in a copper box to provide electric and optical screening. The front end electronics uses the BGO pre-amplifier modified to have a higher gain [3].

## 3 Test-beam results

Two beam tests (in 1994 and in 1995) were performed on module prototypes. The aim of the first test was to study the detector performances at high energy and to compare different types of fibers. Preliminary results from this test have been already reported in [4]. The second one was performed to study the final configuration at lower energies, where detector behaviour is more critical.

### 3.1 1994 Test-beam

The first test was performed at the X3 beam at CERN SPS, with electron energies between 4 and 50 GeV. The trigger was given by the coincidence of 4 scintillators, with the smallest one ($0.5 \times 0.5 cm^2$) located in front of the brick, and a veto counter. Two Čerenkov counters were used to separate electrons from pions and muons up to 10 GeV. Linearity was studied using two modules with Pol.Hi.Tech 0042/1-100 fibers (aluminized at one end) and different beam energies. In order to minimize the effects due to light collection, the beam was pointed to the center of one phototriode. The linearity of the calorimeter response can be seen in Fig. 4 which shows detector pulse height as a function of beam energy.

A comparison of different fiber types, based on light output and energy resolution, lead to the choice of Kuraray SFCS/81 fibers, aluminized at one side.

### 3.2 1995 Test-beam

In 1995 a test was performed at the T7 beam at the CERN PS, a mainly hadronic beam with an energy range of 0.5-10 GeV. The trigger system was similar to that of 1994 test, and electron identification was provided by a single Čerenkov counter.

Three full modules were placed on a mechanical structure simulating the final configuration inside the L3 experiment, and allowing a horizontal and vertical scan of the detector. The modules were inclined with respect to the beam axis to reproduce their final orientation inside L3.

At lower energy the calorimeter linearity was proven to be good, as shown in Fig. 5. The deviation from linearity of the point at 7.5 GeV of beam energy is due to the rear shower leakage caused by the inclination of the modules with respect to the beam, as MonteCarlo study has proved.

After unfolding the beam energy spread of 1%, taken from the beam data sheets for the collimator settings in use, a fit to the energy resolution of the experimental data (Fig. 6) yields

$$\frac{\sigma(E)}{E} = (2.3 \pm 0.6)\% + \frac{(11.6 \pm 1.3)}{\sqrt{E(GeV)}}\%.$$

In order to study the response uniformity as a function of the particle position, we performed a horizontal scan of the modules with beam energy set to 2 GeV (Fig. 7).

Three zones of non uniformity can be seen: the one around 8 cm corresponds to the central part of a module and is caused by some loss of light near the edges of the lightguides, while the ones at 0 and 16 cm are due to the gap between two modules. These non uniformities can be corrected for single particles by calculating the center of gravity of the showers from the signals of two adjacent phototriodes and applying a position-dependent correction to the reconstructed energy.

Fig. 8 shows the reconstructed shower center of gravity in the zone inside a module. Fig. 9 shows the results of the horizontal scan after applying the correction. The non uniformity zone inside a module is completely removed, while the one between two modules is reduced but not eliminated, as part of the energy is lost in the air gap.

We also performed runs with a 5 GeV pion beam in order to test detector response to hadrons and MIPs. The result is shown in Fig. 10, where the signals due to minimum ionizing and strongly interacting pions are clearly visible, above the pedestal. Also shown are particles identified as electrons by the Čerenkov counter

## 4 Monte Carlo simulation

Detector simulation was based on the GEANT [5] package. The modules were described in detail. Each fiber was properly simulated, and the glue layer between fibers and lead was taken into account.

Monte Carlo simulation predicts an energy resolution of:

$$\frac{\sigma(E)}{E} = (0.6 \pm 0.3)\% + \frac{(11.2 \pm 0.6)}{\sqrt{E(\mathrm{GeV})}}\%. \quad (1)$$

in good agreement with data from the 1995 test-beam, concerning the statistical term of the resolution. The constant term is due to the difference in the energy resolution for particles entering the detector in the lead or in the fibers. To reproduce this effect, the beam spot was described as a 2-dimensional gaussian distribution with 5 mm and 1 mm width in the horizontal and vertical directions. These widths are consistent with measurements of the beam spot made with the 1995 test-beam. The results of taking into account the beam spot width in the simulation are an increase in the constant term to 2.2%, in agreement with the experimental results.

Due to the fine structure of the detector, the detailed simulation requires 12 s/GeV on an HP 735. To speed up the simulation, we described the bricks as a mixture of scintillator and lead in the correct ratio. The sampling effect is accounted for rejecting part of the energy released in the brick with a probability given by the sampling ratio. In this way we found a good agreement in the results given by the two MC methods, while the time needed to simulate electromagnetic showers is decreased to 0.01 s/GeV.

In order to take into account the light collection effect, we simulated the light guide efficiency using a ray-tracing technique. The results are in agreement with the measurements described before. A map of simulated lightguide efficiency was then applied to the detector MC simulation. The result of a simulated horizontal scan of a detector module is shown in Fig. 11. The non-uniformity zone inside the module is correctly reproduced.

The whole detector has been simulated inside the L3 frame, allowing the study of the global detector performances.

Fig. 12 shows the energy collected by the BGO calorimeter as a function of the angle with respect to the beam axis for 5 GeV photons pointing into the gap region. Fig. 13 shows the energy that is predicted by summing up the BGO energy and the signal in the lead-scintillating fibers calorimeter, multiplied by the proper intercalibration factor, to account for the sampling. The distribution of the total measured energy (Fig. 14) shows that only 2% of the 5 GeV photons with $38^\circ < \theta < 42^\circ$ deposit less than the estimated energy threshold of the calorimeter of 200 MeV.

## 5 Summary and conclusions

We have reported results on linearity, energy resolution and light collection efficiency for a prototype of the lead-scintillating fiber calorimeter to be used in the L3 experiment. We found that the stochastic term of the resolution is $11.6\%/\sqrt{E(GeV)}$. Based on the test results we also simulated the global characteristics of the detector, showing that, in spite of the space left between the modules, the detector acts as a veto with 98% efficiency.

The full detector will be installed in L3 during the 1995-1996 winter shutdown, and it will be ready for the first phase of LEP2 running.

## References

[1] L3 Collab., B. Adeva *et al.,* Nucl.Inst.Meth. **A 289** (1990) 35.

[2] J. Ellis, D. Nanopulos, S. Rudaz, **Nucl. Phys. B202** , 43 (1982),
G. Costa *et al.*, **Nucl. Phys. B297**, 244 (1988),
J. Ellis, S. Kelley, D. Nanopulos, **Phys. Lett. B260** , 131 (1991).
[3] M.Goyot *et al.*, Nucl.Inst.Meth. **A263** (1988) 180-187.
[4] G.Basti *et al.*, Nuclear Physics B (Proc. Suppl.) **44** (1995) 132.
[5] R. Brun *et al.*, "GEANT 3", CERN DD/EE/84-1 (Revised), September 1987.

**List of Figures**

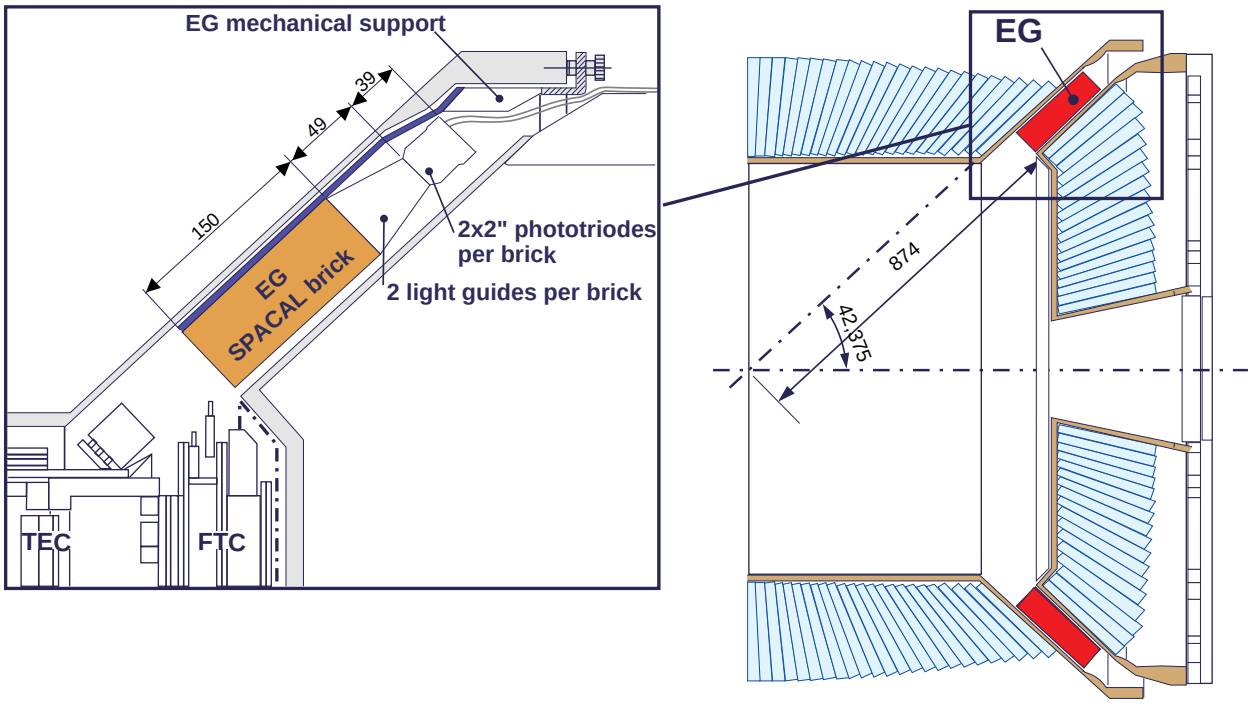


Figure 1: The new calorimeter inside L3

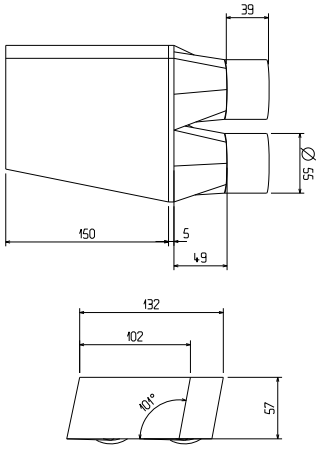


Figure 2: Top and front view of a module

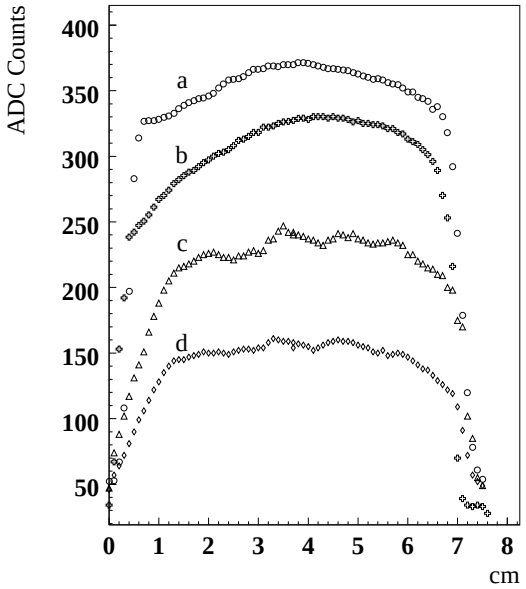


Figure 3: Light collection of different lightguides as a function of horizontal position: a: plexiglass lightguides; b: plastic aluminized guides; c: plastic aluminized lightguides with a Fresnel lens in front; d: plastic aluminized lightguides with Fresnel lens and a glass diffusor.

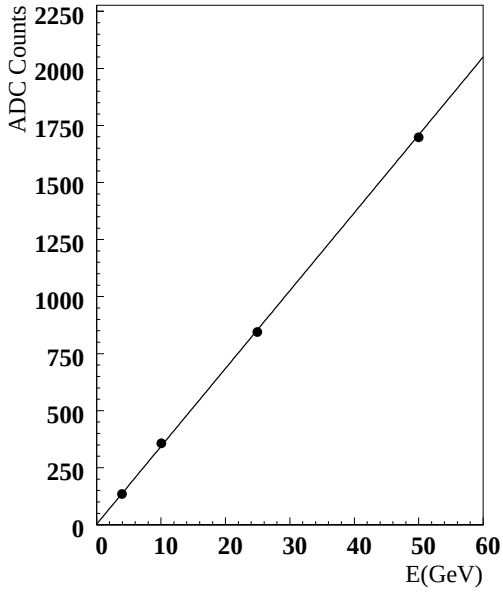


Figure 4: Measured pulse height versus beam energy in 1994 test-beam.

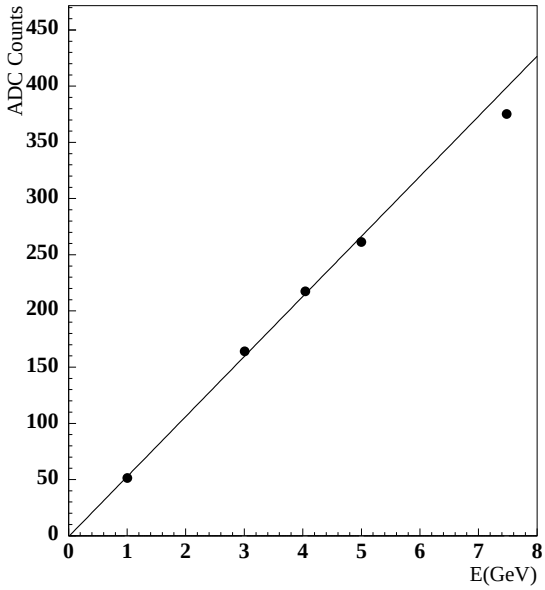


Figure 5: Measured pulse height versus beam energy in 1995 test-beam.

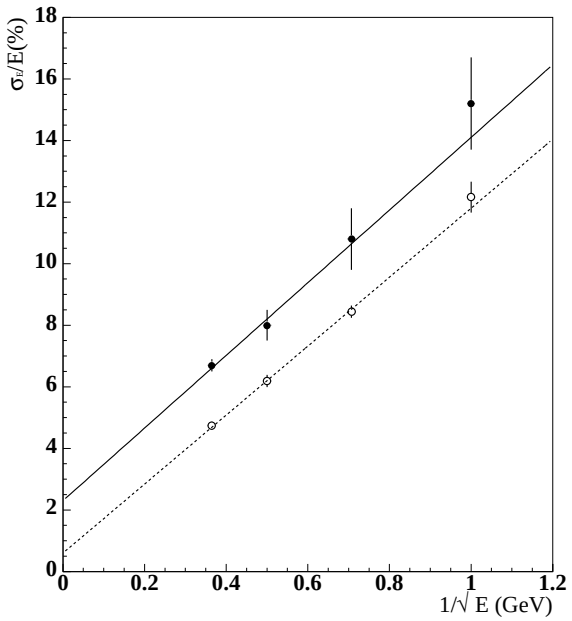


Figure 6: Measured calorimeter resolution in 1995 test-beam (upper line) compared to MC expectation without beam smearing (lower line).

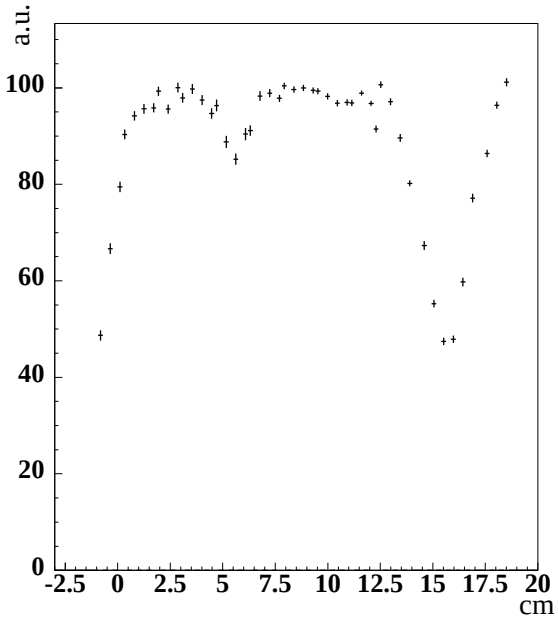


Figure 7: Position dependent response of the detector from an horizontal scan of two adjacent calorimeter modules in the final geometry.

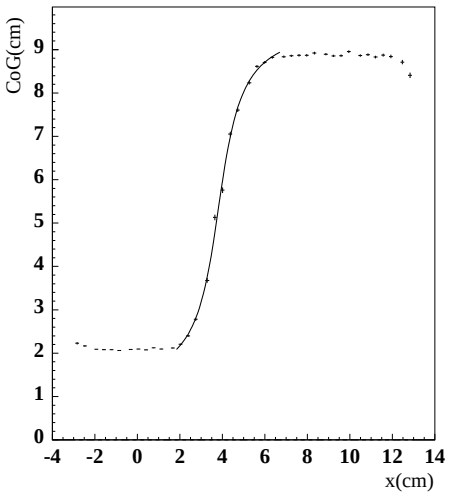


Figure 8: Reconstructed center of gravity as a function of the beam position.

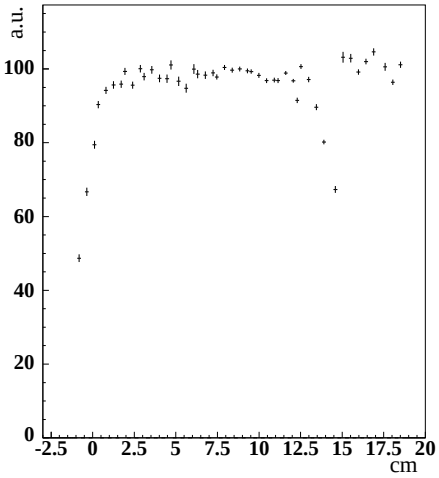


Figure 9: Reconstructed energy after a correction depending on the shower center of gravity.

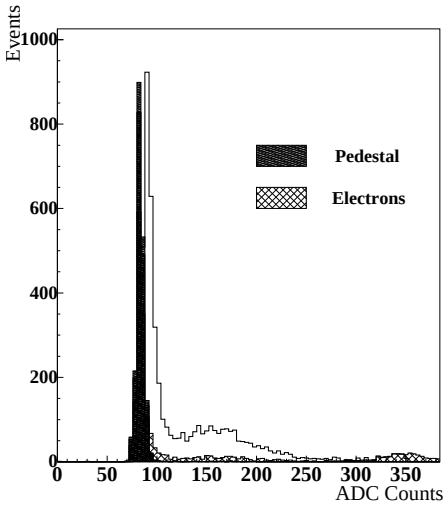


Figure 10: Detector response to a 5 GeV pion beam.

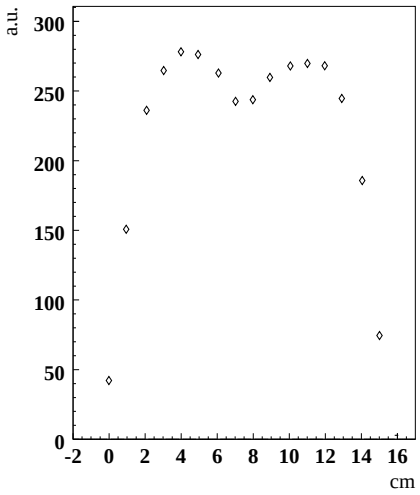


Figure 11: Position dependent detector response from a simulation of an horizontal scan.

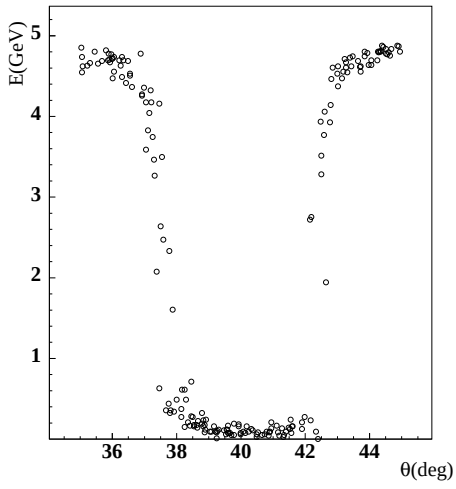


Figure 12: Energy reconstructed by the BGO calorimeter in the gap region.

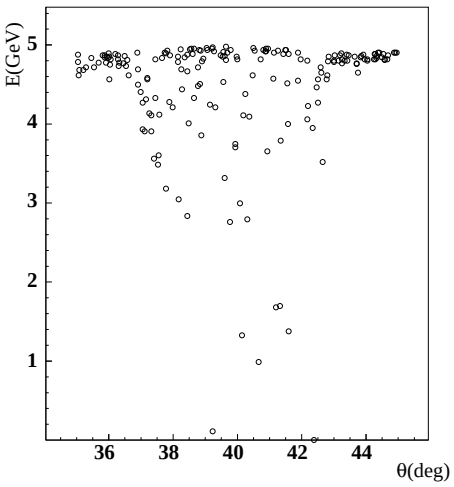


Figure 13: Energy reconstructed by the sum of the BGO and the lead-scintillating fibers calorimeter as a function of polar angle, as predicted by MC simulation.

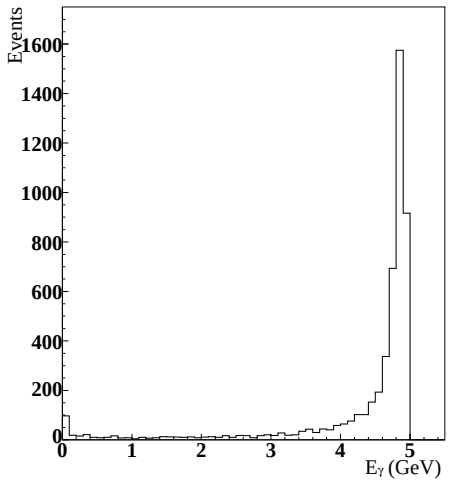


Figure 14: Distribution of the sum of the energis recorded by the BGO and lead-scintillating fibers calorimeters, for the angular range $38^\circ < \theta < 42^\circ$ as predicted by MC simulation.